Int. J. Environ. Sci. Technol. (2015) 12:885–892
DOI 10.1007/s13762-013-0450-6

ORIGINAL PAPER

Phosphorus removal from aqueous solutions containing low concentration of phosphate using pyrite calcinate sorbent

T.-H. Chen · J.-Z. Wang · J. Wang · J.-J. Xie · C.-Z. Zhu · X.-M. Zhan

Received: 19 June 2013 / Revised: 14 September 2013 / Accepted: 20 November 2013 / Published online: 8 January 2014

Abstract Natural pyrite was modified by calcination under nitrogen (N_2) atmosphere to produce a novel sorbent for removing phosphorus (P) with low concentration from aqueous solutions. The crystallinity, porous texture, magnetic susceptibility and performance in P removal of pyrite calcinates depended on calcination temperatures. The sorbent obtained at calcination temperature of 500–600 °C possessed the most efficient P removal. Solution pH in the range of 3.0–9.0 and anions of chloridion (Cl^-), nitrate $(NO_3)^-$ and sulfate (SO_4^{2-}) had ignorable effect on P removal. The batch adsorption experiment shows that the maximum sorption capacities for P of this novel sorbent (q_m) were up to 1.61–5.36 mg P/g at adsorption temperatures of 15–35 °C. Dynamic sorption and regeneration experiments were conducted in an adsorption column filled with pyrite calcined at 600 °C. The study found that oxygen was an important control factor responsible for P adsorption because the oxidization of Fe^{2+} to Fe^{3+} on the surface of the sorbent followed by P being bound to a ferric hydroxide surface film was the crucial processes. The mechanism was confirmed with surface characterization techniques including field emission scanning electron microscope and X-ray photoelectron spectroscopy. This research potentially provides a cheap, abundant sorbent for P removal from the secondary effluent of municipal wastewater treatment plant.

Keywords Calcinations · Low concentration of phosphate · Pyrite · Removal efficiency

Introduction

Recently, a big challenge for Chinese government is how to tackle the shortage of clean freshwater caused by ongoing eutrophication in water bodies. Usually, eutrophication in aquatic ecosystems is caused by the accumulation of phosphorus (P). Municipal wastewater and agricultural application of fertilizer are the main sources of P released into aqueous ecosystems. Despite that numerous chemical and biological approaches have been used for removal of P from wastewaters in wastewater treatment plants, the concentration of P in the treated wastewater is still not low enough; after discharged into water bodies, it can cause excessive algae growth in lakes and other confined water bodies. Currently, 0.5 mg/L is the state emission standard for P in the effluent of municipal wastewater treatment plants (Ministry of Environmental Protection of the People's Republic of China. 2003), which is much higher than the acceptable level of total inorganic P (~0.03 mg/L) in the water environment (Khan and Ansari 2005). Conventional chemical precipitation using calcium, aluminum and iron salts has been widely used for P removal from wastewater. However, they cannot be widely adopted because of high chemical cost and generation of a large volume of chemical sludge, which are considered as the secondary pollution (Clark et al. 1997). In addition, both conventional biological nutrient removal and precipitation processes are not able to reduce the effluent total P concentrations to below 0.2 mg/L (Jenkins et al. 1971). In order to

Electronic supplementary material The online version of this article (doi:10.1007/s13762-013-0450-6) contains supplementary material, which is available to authorized users.

T.-H. Chen (✉) · J.-Z. Wang · J. Wang · J.-J. Xie · C.-Z. Zhu · X.-M. Zhan
School of Resources and Environmental Engineering, Hefei University of Technology, Hefei 230009, China
e-mail: chentianhu@hfut.edu.cn

X.-M. Zhan
Civil Engineering, College of Engineering and Informatics, National University of Ireland, Galway, Ireland

meet high water quality standards for discharge into water bodies or reuse the treated wastewater, novel technologies are required for P removal from the secondary effluent in wastewater treatment plants.

Sorption with ion exchangers and other adsorbent materials is one of the techniques which would be best available technologies. Commercial ion exchange resins (Wu et al. 2007) have outstanding adsorption properties, but have high cost. The application of low-cost and easily available materials in wastewater treatment, including industrial waste solid (Atar and Olgun 2009; Atar et al. 2012; Olgun and Atar 2009; Olgun and Atar 2011; Olgun et al. 2013), bentonite (Haghseresht et al. 2009), activated red mud (Liu et al. 2007), gas concrete (Oğuz et al. 2003) and calcite (Karageorgiou et al. 2007), has been widely investigated in recent years.

Iron sulfide minerals are the most abundant metal sulfide minerals at the surface of the earth and formed in reducing environments. Dissolved iron, sulfate and heavy metals are released as a result of oxidation of iron sulfides when exposed to air, leading to acid mine drainage (AMD). AMD causes severe environmental pollution problems. Recovery of iron sulfides in rock and ore as well as utilization is very important for reducing AMD from the source. Use of iron sulfide minerals and synthetic iron sulfide as sorbents for wastewater treatment and as reducers for remediation of groundwater pollution has received significant attention (Jeong et al. 2007), in particular pyrite and pyrrhotite, which are usually produced during flotation of sulfide ore and are only used as raw materials for production of sulfuric acid (Bower et al. 2008). Janzen et al. (2000) observed the rate of pyrrhotite oxidation at atmospheric concentrations of O_2 was 100 times as much as that of pyrite because there is an S–S double bond in the crystal structure of pyrite and there are structure defects in the crystal structure of pyrrhotite. However, the crystal's sizes of natural iron sulfide minerals are several millimeters in rock or ore, or 0.05–0.1 mm in flotation products, resulting in low specific surface areas and low sorption capacities for wastewater treatment.

Phase transformation of pyrite can occur by calcination at different temperatures. In inert atmosphere (nitrogen, argon and helium) at high temperature, pyrrhotite, a non-stoichiometric iron sulfide, is the most dominant product of pyrite calcination (Bhargava et al. 2009). Previous research has revealed that not only pyrite is transformed into pyrrhotite after calcination in N_2 atmosphere, but also the crystal size of the calcinate is becomes nanometer or submicron (Lambert et al. 1998). The structure of pyrrhotite transformed from pyrite by heat treatment in inert atmosphere is both polycrystalline and porous, resulting in a much higher specific surface area than that of natural pyrrhotite.

To date, there have been no reports about P removal with pyrite calcinate. Therefore, a series of batch and column experiment were carried out in Hefei University of Technology, China, during the year of 2010 to investigate factors affecting the efficiency of pyrite cinated under N_2 atmosphere in P removal from wastewater and to analyze the mechanisms.

Materials and methods

Materials

All experimental reagents used in the present study were of analytical grade unless especially noted. The stock solution of P was prepared by dissolving KH_2PO_4 in distilled water. The concentrations of PO_4^{3-} ranged from 0.5 to 10 mg/L (defined as mg P/L), and the pH value of the solution was adjusted by using 0.1 M NaOH and 0.1 M HCl solutions according to the experiment requirement.

Pyrite calcination

Pyrite was collected from Xinqiao Mine at Tongling City in Anhui Province, China. In the laboratory, it was crushed and sieved into the desired particle sizes of 0.063–0.074 mm and 0.15–0.30 mm, and then rinsed in the reaction cell with 1 % HCl for 3 h to remove carbonate and the iron oxide film formed on the pyrite surface. The samples were then washed several times with distilled water and dried at 100 °C in an anoxic cell. The cleaned pyrite particles were calcined in N_2 atmosphere at 300, 400, 500, 550, 600, 700, 800 or 900 °C for 1 h. The calcinate with diameter of 0.063–0.074 mm was utilized in the batch sorption experiments, while the calcinate with diameter of 0.15–0.30 mm was used in the column sorption experiment in order to have a rapid flow rate in the adsorption columns. The calcination products were characterized by X-ray diffraction (XRD) in the range of 5–70° using a powder diffractometer (Rigaku Corporation, Japan) with Cu $K\alpha$ radiation, the tube voltage 40 kV and the current 100 mA.

Batch sorption experiments

A total of 50 mg/L of phosphorus (referred as 50 mg P/L, equivalent to 220 mg/L of KH_2PO_4) was prepared by analytical grade of potassium dihydrogen phosphate supplied by Shanghai Hengxin Chemical Reagent Co., Ltd. The initial pH of the solution was adjusted by adding 0.1 M HCl or 0.1 M NaOH. All batch sorption experiments were conducted with a constant solid-to-liquid ratio (S/L = 2.0 g/L). Briefly, a known amount of the calcinated particles (0.5 g) with the particle size of 0.063–0.074 mm were added to 300-mL flasks, in addition with 250 mL of with 0.5 mg P/L solution. Once the desired reaction time was reached, the suspensions were separated by centrifugation with a relative centrifugal force of 3,790×g for 15 min. The supernatant was analyzed

for P concentrations. Firstly, sorbents obtained at different calcination temperature (including natural pyrite particles) were investigated the removal efficiency of P in the batch adsorption experiments at the initial pH = 7.0, and the flasks were shaken at 160 rpm in a water bath shaker for 24 h at ambient temperature. Second, the sorbent obtained at 600 °C was chosen to perform the following experiments (1). dynamic experiments: in order to investigate the time for reaction equilibrium, after adding 0.5 g of sorbent and 250 mL of 0.5 mg P/L at ambient temperature, and the initial pH was kept at 7.0, the flasks were shaken mechanically at 0.5, 1, 2, 4, 6, 8, 14, 15, 16, 18 and 24 h; (2), adsorption isotherms experiments: with the purpose of investigation on the initial concentration of adsorbate and the reaction temperature as a function of the P removal, the initial concentrations of P were designed at 0.5, 2, 5, 8, 10, 15 mg P/L, and the reaction was finished at 15, 25 and 35 °C with the initial pH = 7.0 and the reaction time = 24 h; (3), the influence of initial pH and anions on the adsorption: In order to assess the influence of solution pH on P removal, the initial pH values ranged from 3.0 through 12.0 with the initial concentration of p = 0.5 mg P/L, and reaction time = 24 h at ambient temperature. Anions including nitrate, chloride and sulfate at 0.01, 0.05, 0.1, 0.5 and 1.0 M added to the solution; (4), dependence of P sorption by calcined pyrite on oxygen was investigated in four flasks where 250 mL of 0.5 mg P/L solution was added as well as 0.5 g of 0.063–0.074 mm pyrite calcined at 600 °C. Anoxic experiment was carried out in glove box of no oxygen. The supernatant was extracted 2 mL using a syringe every 2 h for 0.5 mg/L P. All batch experiments were performed in triplicate.

Column experiments

A column sorption experiment was conducted at room temperature in a column constructed from a glass pipe with a height of 50 mm and an internal diameter of 10 mm (Fig. 1). The system was located at the base of the column (near the inlet) to evenly distribute the influent flow. The column was filled with 50 g of pyrite calcined at 600 °C with size of 0.15–0.30 mm. The influent solution used in the column experiment contained 1.0 mg P/L with a pH value of approximately 7. During the experiment, the influent was continuously pumped from the medium reservoir tank to the bottom inlet of the column with a pre-calibrated variable-speed peristaltic pump at a flow rate of approximately 17 mL/h. The column effluent was collected and filtered through 0.45-μm membrane filter paper before analysis. The breakthrough P concentration was set at 0.01 mg/L. The reasons are as follows: firstly, many lakes in China, such as Chaohu Lake, Taihu Lake and Dianchi Lake, are seriously eutrophic, and municipal sewage should be treated to a higher standard before discharge; secondly, if the secondary effluent of municipal

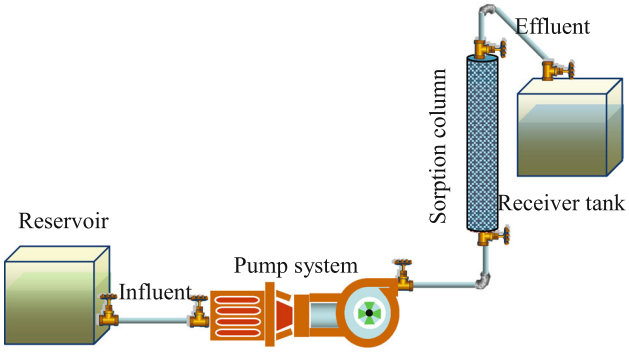

Fig. 1 Schematic diagram of the column sorption experiment

wastewater treatment plants is reused as a city surface water, the P concentration of the secondary effluent has to reach the quality standard of surface water.

To investigate the possibility of reuse of the sorbent, a regeneration experiment was conducted. A solution containing 0.1 M HCl and 0.5 M Na_2SO_3 was pumped into the column at the flow rate of 17 mL/h after breakthrough occurred. The phosphate content of the column elute was measured. Then the column was used to treat the 1.0 mg P/L solution with the protocol for the column experiment described above.

Analysis and characterization

Phosphate concentrations in all solutions were analyzed by a spectrophotometer at a wavelength of 700 nm according to reference (American Public Health Association 1985). In the batch adsorption experiment, the P removal efficiency (RE) was calculated according to Eq. (1):

$$\mathrm{RE}\,(\%) = \frac{C_0 - C_t}{C_0} \times 100 \quad (1)$$

Here, C_0 is the initial concentration of P, and C_t is the concentration of P at adsorption time tth.

At the end of the adsorption experiment, the sorbent material was washed repeatedly there times with distilled water, and then dried in N_2 atmosphere at 30 °C for 12 h before characterization by field emission scanning electron microscope (FE-SEM) and X-ray photoelectron spectroscopy (XPS) to investigate the change of the surface morphology and composition of pyrite calcinate before and after adsorption experiments. XPS were performed using a Thermo ESCALAB 250 XI system equipped with monochromatic Al Kα source (150 W, hν = 1,486.6 eV) at University of Science and Technology of China. The binding energy scale was charge-referenced to the C 1 s peak at 284.8 eV. High-resolution spectra were obtained using analyzer pass energy of 20 eV. The FE-SEM analyses were carried out in the Structural Analysis Center of the University of Science and Technology of China with Sirion 200 FE-SEM.

Results and discussion

Structure and property of pyrite calcinated

The dominant peaks in XRD pattern of the samples obtained at calcination temperature <500 °C were attributed to pyrite and quartz (Fig. S1), and the pyrrhotite peaks were observed for samples calcinated at 500–800 °C, indicating that the transformation of pyrite under N_2 did not occur until the temperature was raised to 500 °C. The already detected products of pyrite calcination are monoclinic pyrrhotite (pyr-M), hexagonal pyrrhotite (pyr-T) and orthogonal troilite (Lambert et al. 1998). When the calcination temperature was 550–600 °C, the predominant product was pyr-M; when the temperature reached 700 °C, pyr-T was the dominant product; troilite, the stoichiometric iron sulfide (FeS), was the main product over 800 °C (Fig. S1). Accordingly, in crystallography, simple cubic crystal system was transformed to monoclinic or hexagonal crystal symmetry. Transformation of pyrite to pyrrhotite is endothermic and can be expressed by the chemical equation as follows (Bhargava et al. 2009):

$$\mathrm{FeS_2(s)} \overset{500-600^{\circ}\mathrm{C}}{\longrightarrow} \mathrm{FeS}_x\mathrm{(s)} + (1+0.5x)\mathrm{S_2(g)} \overset{700-900^{\circ}\mathrm{C}}{\longrightarrow} \mathrm{FeS(s)} + \mathrm{S(g)} \quad (2)$$

The value of x in FeS_x is only a function of temperature (Li and Franzen 1996).

Significant difference in removal of phosphate from aqueous solutions was observed for pyrite calcined at different temperatures (Fig. S2). High removal efficiencies (from 89.7 to 96.2 %) were achieved by pyrite calcined at 500–600 °C. The highest P removal efficiency, up to 96.2 %, was obtained for pyrite calcined at 600 °C. The effect of calcination temperature on P removal efficiency can be explained in terms of the phase composition in the calcinates: The main component of pyrite calcinate at 500–600 °C is Pyr-M. Pyr-M with wide and weak peaks in XRD patterns implies its low crystallinity, with crystal sizes ranging from nanometer to submicron meter. The crystallinity of pyr-M formed from pyrite calcination was lower than that of natural pyrrhotite. Furthermore, pyrite calcined at 500–600 °C had a surface area about 10 m^2/g (tested using the BET-N_2 adsorption method), while the surface area of original pyrite particle was less than 0.02 m^2/g (calculated according to the granular size). The increased specific surface area of pyrite calcinated at 500–600 °C was due to its porous texture with submicron crystal sizes of monoclinic pyrrhotite (Fig. 2). Previous studies also demonstrated that among iron sulfides (pyrite, marcasite, pyr-M, pyr-T, orthogonal troilite and tetragonal mackinawite), pyr-M had the highest chemical activity for oxidation by dissolve oxygen or air (Janzen et al. 2000; Lehmann et al. 2000; Thomas et al. 2003).

Additionally, the arsenic content in the calcination products of pyrite was reduced as the increase in the calcination temperature. The magnetic susceptibility of pyr-M was the highest among the iron sulfides (Fig. S2). Therefore, the high magnetic susceptibility, specific surface area, chemical activity and the low arsenic content can be obtained through the calcination of pyrite at N_2 atmosphere.

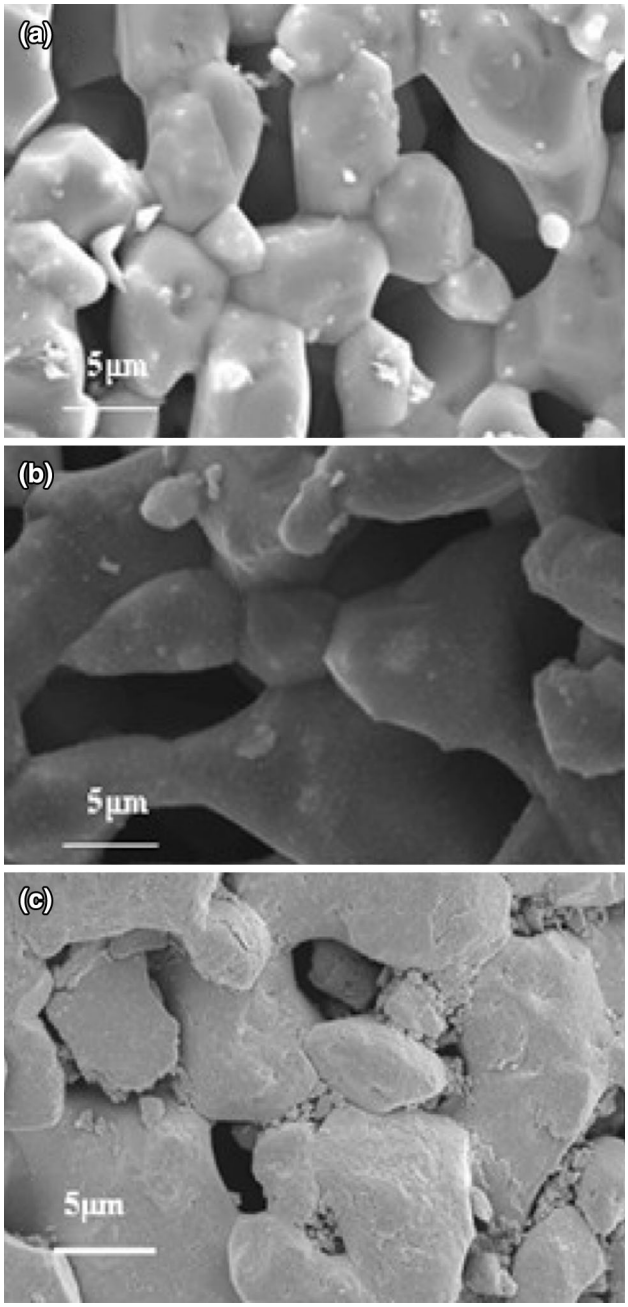

Fig. 2 FE-SEM images of sorbent particles **a** before adsorption, **b** after immersion in P solutions under anoxic conditions and **c** under oxic conditions

Removal kinetics and sorption isotherms

P was removed slowly within the first 2 h in the batch adsorption experiment, and then, P concentrations in the

aqueous solutions were rapidly decreased. The adsorption was nearly complete within 6 h (Fig. S3a). The removal efficiency of P was ~98 % after 6 h of adsorption. Generally, sorption kinetics of P by iron oxides can be described with first-/second-order kinetic models (Hamdi and Srasra 2012). However, P removal by pyrite calcinate did not fit well with either first-order or second-order kinetic models. This possibly resulted from the multi-step reactions and chemical adsorption between pyrite calcinate and P. Briefly, these chemical reactions would consist of oxidization of Fe^{2+} (Eq. 3) on the sorbent surface, reactions between Fe^{3+} and OH^- (Eq. 4) and sorption of orthophosphate by the newly formed ferric hydroxide (Eq. 5). $H_2PO_4^-$ and HPO_4^{2-} were the main species under pH and P concentrations used in this study according to the computation of hydrolysis balance constants.

$$2Fe^{2+} + O_2 + 4H^+ \rightleftharpoons 2Fe^{3+} + 2H_2O \quad (3)$$

$$Fe^{3+} + 3H_2O \rightleftharpoons Fe(OH)_3 + 3H^+ \quad (4)$$

$$S-Fe-OH + H_2PO_4^- \rightarrow S-Fe-HPO_4^- + H_2O \quad (5)$$

Equation 3 is an O_2-dependent reaction. The results from batch experiments under anaerobic and aerobic conditions confirm the importance of oxygen for the phosphate removal (Fig. S3b and c). P was not removed by calcined pyrite under anaerobic conditions within 16 h of experiment (Fig. S3b), while it was obviously removed under aerobic conditions (Fig. S3c), indicating that O_2 would be one of the most important factors causing P removal by calcined pyrite. Despite that non-oxidative dissolution of iron sulfides could occur in acidic solutions (Nicol and Scott 1979), the mean oxidation rate of pyrrhotite by oxygen was about two orders of magnitude faster than that of non-oxidative dissolution in solutions with pH of 2.75 (Janzen et al. 2000). Therefore, non-oxidative dissolution was not a key factor to P removal in the present study. FE-SEM images of calcined pyrite before and after contact with the P solution confirm our conjecture (Fig. 2b, c). There were no obvious changes on the surface of crystals in comparison with fresh surface of pyrite calcinate after being contacted with 0.5 mg P/L solution under the anaerobic condition (Fig. 2b). However, there was a new film of ferric hydroxide containing P formed on the surface of crystals after being contacted with P solution under the aerobic conditions (Fig. 2c). As mentioned earlier, existence of oxygen could oxidize Fe^{2+} to Fe^{3+} which was easy to produce a film of ferric hydroxide. Ferric hydroxide was demonstrated the key factor in adsorption (Jain et al. 1999; Raven et al. 1998; Roberts et al. 2003). Therefore, our results also confirm that ferric hydroxide film formed due to the surface oxidation of the particles under the oxic condition caused the P sorption from the solution onto the sorbent surface. As a result, P removal by calcined pyrite was a series of complicated processes, and the overall removal of P could not be described by first- or second-order kinetic models.

Table 1 Estimated isotherm parameters for P adsorption by calcined pyrite

	Equation	R^2	SE
Freundlich equation	$q = KC^{\frac{1}{n}}$		
15 °C	$q = 0.746C^{\frac{1}{3.27}}$	0.86	0.22
25 °C	$q = 0.893C^{\frac{1}{3.38}}$	0.92	0.19
35 °C	$q = 1.62C^{\frac{1}{2.09}}$	1.0	0.06
Langmuir equation	$q = \frac{bq_mC}{1+bC}$		
15 °C	$q = \frac{0.996 \times 1.61C}{1+0.996C}$	0.98	0.08
25 °C	$q = \frac{1.54 \times 1.75C}{1+1.54C}$	0.99	0.08
35 °C	$q = \frac{0.395 \times 5.36C}{1+0.395C}$	0.99	0.12
Temkin equation	$q = A + B\ln C$		
15 °C	$q = 0.789 + 0.309\ln C$	0.95	0.13
25 °C	$q = 0.978 + 0.324\ln C$	0.98	0.09
35 °C	$q = 2.18 + 0.617\ln C$	0.87	0.57
Redlich–Peterson equation	$q = \frac{aC}{1+bC^n}$		
15 °C	$q = \frac{1.17C}{1+0.485C^{1.17}}$	0.99	0.06
25 °C	$q = \frac{3.04C}{1+1.91C^{0.956}}$	0.99	0.09
35 °C	$q = \frac{27.2C}{1+15.7C^{0.549}}$	1.0	0.06
Langmuir–Freundlich equation	$q = \frac{bq_mC^{\frac{1}{n}}}{1+bC^{\frac{1}{n}}}$		
15 °C	$q = \frac{1.48 \times 1.22C^{\frac{1}{0.7}}}{1+1.48C^{\frac{1}{0.7}}}$	0.99	0.06
25 °C	$q = \frac{1.74 \times 1.6C^{\frac{1}{0.975}}}{1+1.74C^{\frac{1}{0.975}}}$	0.99	0.09
35 °C	$q = \frac{0.113 \times 15.9C^{\frac{1}{1.76}}}{1+0.113C^{\frac{1}{1.76}}}$	1.0	0.04

The sorption data for P removal at temperatures of 15, 25 and 35 °C were correlated using five equation models (Table 1; Fig. 3). Langmuir, Redlich–Peterson and Langmuir–Freundlich models are more suitable for describing the sorption isotherms than Freundlich and Temkin models based on their higher R^2 and less standard error of estimate (SE). P maximum sorption capacities (q_m) calculated from Langmuir and Langmuir–Freundlich models were up to 1.61 and 1.22 mg P/g sorbent at 15 °C, 1.75 and 1.6 mg P/g at 25 °C, and 5.36 and 15.9 mg P/g at 35 °C, respectively. With the adsorption temperature increasing, the sorption capacity was increased. A previous study also indicated that the oxidative reaction rate of pyrrhotite increased with increasing the solution temperature (Van Weert et al. 1974). Therefore, P removal by calcined pyrite is dependent on the temperature.

Effect of pH and anions on P adsorption

pH is an important factor that affects the sorption of anions and cations at the solid–liquid interface. When pH is from 3.0 to 7.2, the predominant phosphate species in aqueous solutions is $H_2PO_4^-$, while at pH between 7.20 and 12.33, the main phosphate species is HPO_4^{2-} (Perrin and Dempsey 1974). The

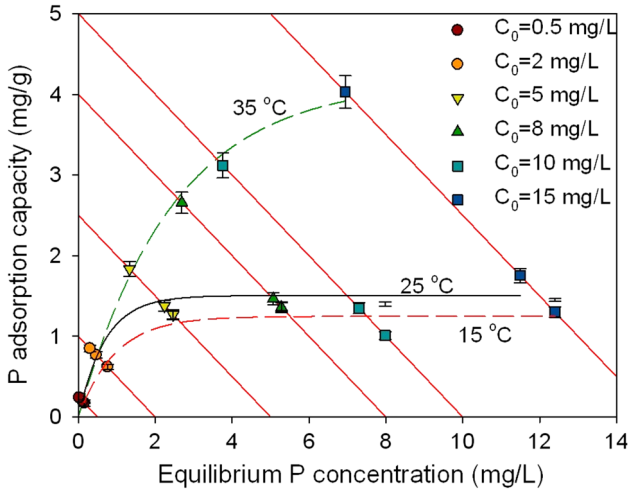

Fig. 3 P adsorption isotherm of calcined pyrite at 15, 25 and 35 °C

removal efficiency of P at varying pH (3.0–12.0) is illustrated in Fig. S4. After the sorption reached equilibrium, pH increased in the batch experiments with initial pH less than 7 and decreased in batch experiments with initial pH higher than 7. The optimal pH range for P removal was from 3.0 to 9.5 had little influence on the removal efficiency (from 95.7 ± 4.4 to 98.0 ± 5.0 %), whereas the efficiency decreased to 42.6 ± 5.6 % at initial solution pH = 12.0. It was due to a proceeding oxidation and hydrolysis step of ferric iron (III) hydroxides (Eqs. 3, 4), which strongly bind P (Parfitt et al. 1975). A decrease in P removal at higher pH was likely due to the high concentration of OH^- ions present in the solution which competed with PO_4^{3-} ions for the sorption sites on the surface of the sorbent.

Wastewater contains a variety of anions which could interfere in the binding of P. Thus, the competitive sorption of the additional anions including nitrate, chloride and sulfate was investigated with 0.5 mg P/L solutions containing 0.01, 0.05, 0.1, 0.5 and 1.0 M NO_3^-, Cl^- or SO_4^{2-} anions (Fig. S5). The results demonstrate that compared with the control experiment where no anions were present in the solutions, and 98.9 % of P removal was achieved, only ignorable interference was observed in the presence of 0.01–1.0 M NO_3^-, Cl^- or SO_4^{2-} anions and P removal efficiency was consistently above 96 %. Competition sorption by anions has been found on furnace slag[40] and orange waste gel loaded with zirconium (Xue et al. 2009). For iron sulfide, it was also reported that P removal by raw natural pyrite was more strongly affected by SO_4^{2-} ion than by NO_3^- or Cl^- ions (Wang et al. 2012). In the present study, the calcined product was still efficient in P removal in the presence of NO_3^-, Cl^- or SO_4^{2-} anions.

Results of the column sorption and regeneration experiments

The P concentration in the column effluent was analyzed and is presented in Fig. 4 as a function of the accumulative volume of treated influent solution. The results show that when the column breakthrough occurred (the P concentration in the effluent was above 0.01 mg/L), an accumulative volume of 8.6 L was treated by the column, equal to 350 bed volume (BV); the column had been operated for 23.4 days. Prior to this breakthrough point, the amount of P sorbed onto pyrite calcined was 0.17 mg/g sorbent that was computed by dividing the amount of P removed in 23.4 days by the filling amount of pyrite calcined in the column. The breakthrough point (P concentration of 0.01 mg P/L) was lower than Grade I National Surface Water Quality Standards in China, 0.02 mg/L (GB3838–2002). From this point of view, pyrite modified is an effective sorbent for reducing P removal to a very low level and can be used for polishing the secondary effluent of the municipal wastewater treatment plants. It is noted that high concentration of P was observed in the effluent during influent volume of 8–12 L, whereas low concentration in the effluent was detected during accumulative volume of 12–14 L. The potential reason for the phenomenon is likely associated with unstable adsorption when adsorption approached saturation. In addition, the concentrations of total Fe, Zn and sulfate in the effluent were below 5, 0.04 and 85 mg/L, respectively, and other heavy metals (Cu, Cd, Pb, Ni, Co, Mn) and As were all below detection limits. The results promise and suggest that there would be little leaching of the trace heavy metals from the calcinate during adsorption of P. It was noted that there was no significant difference in pH between the influent and the effluent during the entire experiment, and pH values remained consistently neutral.

To make the sorbent more economical, regeneration and reuse of the sorbent are necessary. Regeneration studies were carried out using the solution containing 0.1 M HCl and 0.5 M Na_2SO_3, which aided in reduction and dissolution for the ferric hydroxide film containing P on the surface of the sorbent. During regeneration, the P concentration in the column leachate was decreased gradually from 83.3 to 1.53 mg/L after washing for 13 h (Fig. S6a). After regeneration, the column

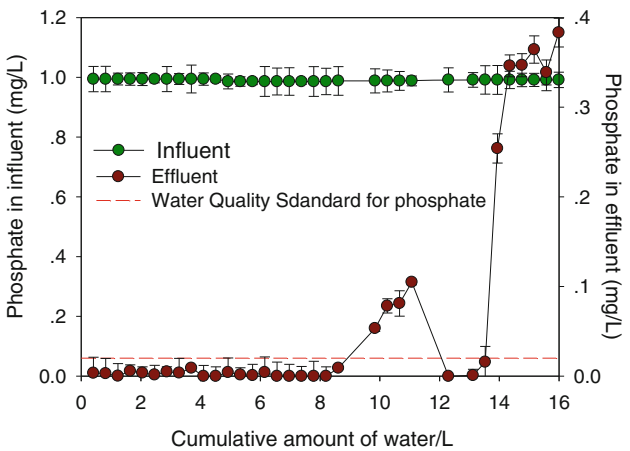

Fig. 4 Performance of the continuous column adsorption experiment

was run again according to the column test procedure mentioned above, and the P sorption capacity calculated was 0.14 mg/g, which was slightly lower than that obtained in the former adsorption test (0.17 mg/g, Fig. S6b), revealing that the sorbent still had a good performance for P removal after regeneration, and the sorbent would be suitable for reuse.

XPS characterization

X-ray photoelectron spectroscopy of calcined pyrite before and after contact with the P solution confirms the analysis of for the P removal mechanism (Fig. S7 and Fig. 5). In the XPS survey spectrum of the calcined pyrite before adsorption, all photoelectron peaks corresponded to Fe, S, O, except the C 1 s photoelectron peak (Fig. S7a). The C 1 s peak was due to CO_2 adsorption when the sample was exposed to air. The O 1 s peak in the fresh sample indicated that oxidation had took place on the surface of the sample before the adsorption experiment started. Comparing with fresh pyrite calcinate, after contacting P solutions, the peaks of O 1 and C 1 s were enhanced, and the peaks of S 2p and Fe 2p were weakened (Fig. S7c). The peak intensity of O 1 s and C 1 s of the surface of samples that contacted P solution under oxic conditions was stronger than on the surface of samples that contacted P solutions under anoxic conditions. The changes of surface composition indicate that calcined pyrite had undergone oxidation reaction in oxic P solution.

Calcined pyrite did not contain P, so there was no P signal in the XPS of the fresh sample (Fig. 5a). P signal in the XPS of the sample contacting anoxic P solution was hardly detected, which is consistent with the finding that the sorption of P on calcined pyrite under anoxic conditions was very low (Fig. S3). The signal of P 2p XPS was strong after calcined pyrite contacted oxic P solutions. Moreover, according to the fine XPS of P 2p (Fig. 5b), the component at 133.75 eV corresponded to the chemical bond of Fe-PO_4^{3-} (Moulder et al. 2004). Fine XPS of S indicated a sensible change in valence of sulfur species by exposure to the oxic solution (Fig. 5c); in particular, S 2p spectra exhibited a second peak at 168.2 eV, which was attributed to SO_4^{2-} groups, indicating that S^{2-} was oxidized in the oxic solution to form SO_4^{2-} (Smart. 1991). The Fe 2p photoelectron peaks shifted to higher binding energy (BE) after contacting with the P solution (Fig. 5c), from 708.3 eV to 711–713 eV. The peak at 708.3 eV was attributed to ferrous property of iron-deficient sulfide groups (Fig. 5c) (Xue et al. 2009). The peak at 711–713 eV was attributed to ferric hydroxide (Smart. 1991). The results confirmed surface oxidation of calcined pyrite and formation of ferric hydroxide in the oxic P solution. Sorption experiment and fine XPS of Fe, S and P all indicate that the surface of calcined pyrite was continuously oxidized and ferric hydroxide was continuously formed, which was responsible for the removal of P in aqueous solutions. Parfitt et al. (1975) have proposed that ferric hydroxide had a strong sorption for P. These experimental observations were in agreement with previous geochemical studies that showed P binds strongly to iron (III) hydroxides and oxides (Davis and Kent 1990).

In summary, the ferric hydroxide formed during oxidation of pyrite calcinate by oxygen dissolved in wastewater would determine the sorption of P from wastewater. The formation rate of ferric hydroxide was controlled by the oxidation rate of pyrite calcinate. In turn, the oxidation rate, i.e., the chemical reactivity of the pyrite calcinate, would determine the efficiency of P removal. The product of pyrite calcination at 600 °C comprised monoclinic pyrrhotite with low crystallinity and porous texture. The calcination of pyrite under N_2 atmosphere enhanced the chemical reaction activity, causing the calcinate being more active than natural pyrite and pyrrhotite. Considering the performance of pyrite calcinate for P removal, abundant pyrite resource as well as low costs of pyrite and pyrite calcination, the new material has a great potential for P removal from the secondary effluent of municipal wastewater treatment plants, as well as recovery of P.

Conclusion

The product of pyrite calcined in N_2 atmosphere at 600 °C is single monoclinic pyrrhotite, low crystallinity and porous texture, which has the highest chemical activity among the iron sulfide and efficiency for the removal of trace phosphate in aqueous solutions. Phosphate uptake was weakly affected

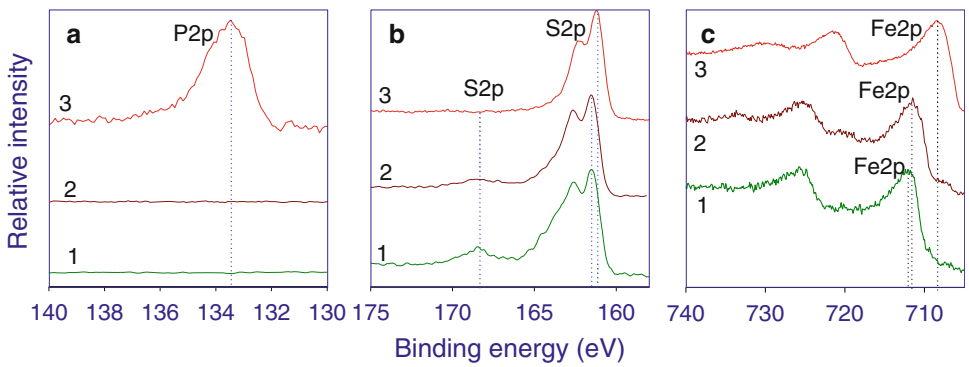

Fig. 5 High-resolution XPS spectra of P 2p (**a**), S 2p (**b**) and Fe 2p (**c**). *Line 1* represents before adsorption, *Line 2* represents after immersion in P solutions under anoxic conditions, and *Line 3* represents after immersion in P solutions under oxic conditions

by nitrate, chloride and sulfate at the concentration of 1 M and pH 3–11. The phosphate removal efficiency was 96.2 % for an initial concentration of 0.5 mg/L phosphorus with calcined pyrite in N_2 at 600 °C. The maximum sorption capacity of phosphate was 0.17 mg/g (0.02 mg/L P was the upper limit of the effluent) by running the column experiment with the calcined product as filter for removal of low concentrations phosphate ($C_0 = 1.0$ mg/L P). The mechanism of phosphate removal is iron (III) hydroxides irreversibly adsorbs phosphate and forms precipitation of iron phosphate on the surface of monoclinic pyrrhotite because the material surface was oxidized in the oxic environment. The precipitation of iron phosphate in the material surface could be cleared up and regenerated with the solution of 0.1 M hydrochloric acid and 0.5 M sodium sulfite.

Acknowledgments This study was financially supported by the Natural Science Foundation of China (Nos. 41072035, 41102023) and the Specialized Research Fund for the Doctoral Program of Higher Education of China (20110111110003). The authors appreciate the financial support.

References

American Public Health Association, American Water Works Association and Water Environment Federation Standard Methods (1985) Standard methods for the examination of water and wastewater: 16th edition. In: American Public Health Association. 445–446

Atar N, Olgun A (2009) Removal of basic and acid dyes from aqueous solutions by a waste containing boron impurity. Desalination 249:109–115

Atar N, Olgun A, Wang S (2012) Adsorption of cadmium (II) and zinc (II) on boron enrichment process waste in aqueous solutions: batch and fixed-bed system studies. Chem Eng J 192:1–7

Bhargava SK, Garg A, Subasinghe ND (2009) In situ high-temperature phase transformation studies on pyrite. Fuel 88:988–993

Bower J, Savage KS, Weinman B, Barnett MO, Hamilton WP, Harper WF (2008) Immobilization of mercury by pyrite (FeS2). Environ Pollut 156:504–514

Clark T, Stephenson T, Pearce PA (1997) Phosphorus removal by chemical precipitation in a biological aerated filter. Water Res 31:2557–2563

Davis JA, Kent DB (1990) Surface complexation modeling in aqueous geochemistry. Rev Mineral Geochem 23:177–260

Haghseresht F, Wang S, Do DD (2009) A novel lanthanum-modified bentonite, Phoslock, for phosphate removal from wastewaters. Appl Clay Sci 46:369–375

Hamdi N, Srasra E (2012) Removal of phosphate ions from aqueous solution using Tunisian clays minerals and synthetic zeolite. J Environ Sci 24:617–623

Jain A, Raven KP, Loeppert RH (1999) Arsenite and arsenate adsorption on ferrihydrite: surface charge reduction and net OH- release stoichiometry. Environ Sci Tech 33:1179–1184

Janzen MP, Nicholson RV, Scharer JM (2000) Pyrrhotite reaction kinetics: reaction rates for oxidation by oxygen, ferric iron, and for nonoxidative dissolution. Geochim Cosmochim Acta 64:1511–1522

Jenkins D, Ferguson JF, Menar AB (1971) Chemical processes for phosphate removal. Water Res 5:369–389

Jeong HY, Kim H, Hayes KF (2007) Reductive dechlorination pathways of tetrachloroethylene and trichloroethylene and subsequent transformation of their dechlorination products by mackinawite (FeS) in the presence of metals. Environ Sci Tech 41:7736–7743

Karageorgiou K, Paschalis M, Anastassakis GN (2007) Removal of phosphate species from solution by adsorption onto calcite used as natural adsorbent. J Hazard Mater 139:447–452

Khan FA, Ansari AA (2005) Eutrophication: an ecological vision. Bot Rev 71:449–482

Lambert JM, Simkovich JRG, Walker PL (1998) The kinetics and mechanism of the pyrite-to-pyrrhotite transformation. Metall Mater Trans B 29:385–396

Lehmann MN, Kaur P, Pennifold RM, Dunn JG (2000) A comparative study of the dissolution of hexagonal and monoclinic pyrrhotites in cyanide solution. Hydrometallurgy 55:255–273

Li F, Franzen HF (1996) Ordering, incommensuration, and phase transitions in pyrrhotite: Part II: a high-temperature X-ray powder diffraction and thermomagnetic study. J Solid State Chem 126:108–120

Liu C-J, Li Y-Z, Luan Z-K, Chen Z-Y, Zhang Z-G, Jia Z-P (2007) Adsorption removal of phosphate from aqueous solution by active red mud. J Environ Sci 19:1166–1170

Ministry of Environmental Protection of the People's Republic of China (2003) Discharge standard of pollutants for municipal wastewater treatment plant (GB 18918-2002)

Moulder, JF, Stickle, WF and Sobol, PE (2004) Handbook of X-ray photoelectron spectroscopy. In: Perkin-elmer Corporation Publisher

Nicol, MJ, Scott, PG (1979) The kinetics and mechanism of the non-oxidative dissolution of some iron sulphides in aqueous acidic solutions. J South Afr Inst Min Metall 298–305

Oğuz E, Gürses A, Canpolat N (2003) Removal of phosphate from wastewaters. Cem Concr Res 33:1109–1112

Olgun A, Atar N (2009) Equilibrium and kinetic adsorption study of Basic Yellow 28 and Basic Red 46 by a boron industry waste. J Hazard Mater 161:148–156

Olgun A, Atar N (2011) Removal of copper and cobalt from aqueous solution onto waste containing boron impurity. Chem Eng J 167:140–147

Olgun A, Atar N, Wang S (2013) Batch and column studies of phosphate and nitrate adsorption on waste solids containing boron impurity. Chem Eng J 222:108–119

Parfitt RL, Atkinson RJ, Smart RSC (1975) The mechanism of phosphate fixation by iron oxides. Soil Sci Soc Am J 39:837–841

Perrin DD, Dempsey B (1974) Buffers for pH and metal ion control. In: Springer Netherlands

Raven KP, Jain A, Loeppert RH (1998) Arsenite and arsenate adsorption on ferrihydrite: kinetics, equilibrium, and adsorption envelopes. Environ Sci Tech 32:344–349

Roberts LC, Hug SJ, Ruettimann T, Billah MM, Khan AW, Rahman MT (2003) Arsenic removal with iron(II) and iron(III) in waters with high silicate and phosphate concentrations. Environ Sci Tech 38:307–315

Smart RSC (1991) Surface layers in base metal sulphide flotation. Miner Eng 4:891–909

Thomas JE, Skinner WM, Smart RSTC (2003) A comparison of the dissolution behavior of troilite with other iron(II) sulfides; implications of structure. Geochim Cosmochim Acta 67:831–843

Van Weert G, Mah K, Piret NL (1974) Hydrometallurgy. Can Min Metall Bull 97–103

Wang J, Chen T-H, Li P, Xie J–J, Ma B-D, Cao G-Y (2012) Removal phosphate in low concentration by pyrite. Acta Mineralogica Sin 32:238–243

Wu RSS, Lam KH, Lee JMN, Lau TC (2007) Removal of phosphate from water by a highly selective La(III)-chelex resin. Chemosphere 69:289–294

Xue Y-J, Hou H-B, Zhu S-J (2009) Characteristics and mechanisms of phosphate adsorption onto basic oxygen furnace slag. J Hazard Mater 162:973–980